

## Effects of Chemical Modification of Thiol–Ene Networks on Enthalpy Relaxation

Junghwan Shin, Sergei Nazarenko, and Charles E. Hoyle\*

School of Polymers and High Performance Materials, University of Southern Mississippi,  
118 College Drive, Hattiesburg, Mississippi 39406

Received January 21, 2009; Revised Manuscript Received July 20, 2009

**ABSTRACT:** The highly uniform and dense network structure of photopolymerized thiol–enes was chemically modified, and the enthalpy relaxation of the networks was measured. *n*-Alkyl acrylate and hydroxyl acrylate groups were incorporated into thiol–ene networks using a phosphine-catalyzed Michael addition reaction. The effect of flexible alkyl side chains and hydrogen bonding on sub- $T_g$  relaxation was evaluated without sacrificing network uniformity. Overall both the rate and extent of enthalpy relaxation decreased as a function of the flexible *n*-alkyl chain length, while hydrogen bonding resulted in enhanced enthalpy relaxation. A trithiol–triene–triacylate ternary system was investigated by correlating enthalpy relaxation and network uniformity. A multifunctional acrylate (TMPTA), being capable of homopolymerization as well as thiol–acrylate copolymerization, was incorporated into a thiol–ene network structure, thereby decreasing the network uniformity and significantly affecting the enthalpy relaxation behavior. In all cases, the extent and rate of enthalpy relaxation were directly related to the heat capacity change at the glass transition which defines the enthalpic departure from equilibrium at a given temperature below  $T_g$ .

### Introduction

Thiol–ene-based networks have many advantages as a result of the unique reaction mechanism (free-radical step growth) by which they are formed and their uniform, high density molecular structures (Figure 1a).<sup>1–11</sup> The kinetics of formation and physical characterization of thiol–ene networks has attracted much attention during the past decade. Due to their current and future use in a variety of applications as basic network films, there has been considerable interest in characterizing the basis of the thiol–ene networks with several hundred publications in the past 5–7 years, many dealing with applications including nanolithography, microfluidics, gradient films, frontal polymerization, pillar arrays, and nanostructured networks provided herein for reference.<sup>1–21</sup> An important implication of the uniform highly dense thiol–ene network structure on sub- $T_g$  aging properties was recently reported.<sup>22</sup> It was found that considerable enthalpy relaxation upon physical aging was observed within a narrow temperature range with a maximum relaxation rate at about  $T_g - 10$  °C for several thiol–ene films. The extent of the enthalpy relaxation exhibited a linear relationship with the logarithmic annealing time ( $t_a$ ). Both temperature and time dependency of the enthalpy relaxation process were directly affected by two molecular parameters, the network connectivity density, hereafter referred to as the cross-link density, and the flexibility of the chemical units comprising the network. It was reported that the maximum enthalpy relaxation decreased with the rigidity of the ene structure and an increase in cross-link density resulting from an increase in the thiol functionality. Physical aging of polymers below their glass transition temperature involves the densification of chains resulting in an increase in the apparent glass transition temperature and changes in physical properties. Since many thiol–ene systems have glass transitions approximately 10–30 °C above room temperature, it might be expected that potential problems due to changes in physical and mechanical

properties can develop when such materials are aged near room temperature for time periods up to several months.<sup>22</sup>

It is well-known that chain mobility and conformational structure changes of polymer systems that affect enthalpy and volume relaxation during physical aging are dependent on molecular weight and molecular weight distribution for linear polymers, and the cross-link-density and distribution of molecular weight between cross-links for cross-linked polymers.<sup>23–29</sup> It has been shown that molecular mobility in linear polymers can be controlled by structural parameters such as flexible *n*-alkyl side groups substituents<sup>30–32</sup> and hydrogen bonding.<sup>33,34</sup> Flexible *n*-alkyl substituents do not limit backbone rotation of linear polymers, but rather reduce interaction between chains resulting in lowering  $T_g$  by an internal plasticization type of effect.<sup>30</sup> Accordingly, it has been suggested that the *n*-alkyl groups begin movement below  $T_g$  resulting in a concomitant increase in heat capacity in the glassy phase and an overall decrease in the heat capacity change ( $\Delta C_p$ ) at  $T_g$ . This, of course, affects the rate and extent of sub- $T_g$  physical aging by reducing the thermodynamic force, i.e.  $\Delta C_p$ , for relaxation. For polymers containing hydroxyl substituents which are capable of forming hydrogen bonding, inter- or intramolecular interactions increase and, as a result, the thermodynamics/kinetics of physical aging and enthalpy relaxation are largely affected. Enthalpy relaxation and free volume changes in linear polystyrene and modified polystyrene copolymer with hydroxyl substituents have been reported.<sup>33,34</sup> The larger extent of enthalpy relaxation for the copolymer was attributed to an enhanced thermodynamic driving force for relaxation due to a higher heat capacity in the rubbery phase and hence higher  $\Delta C_p$  value at  $T_g$ .

While there have been significant efforts to modify linear polymers and alter their sub- $T_g$  relaxation processes, a systematic chemical structural approach with the intention of restricting or controlling physical aging has not been investigated in detail for thiol–ene networks. A general depiction of a strategy for binding *n*-alkyl and hydroxyl alkyl acrylate groups chemically into thiol–ene networks is shown in Figure 1b. As thiol–ene networks are highly uniform, they are an excellent platform for assessing how chemical structural

\*Corresponding author. E-mail: charles.hoyle@usm.edu.

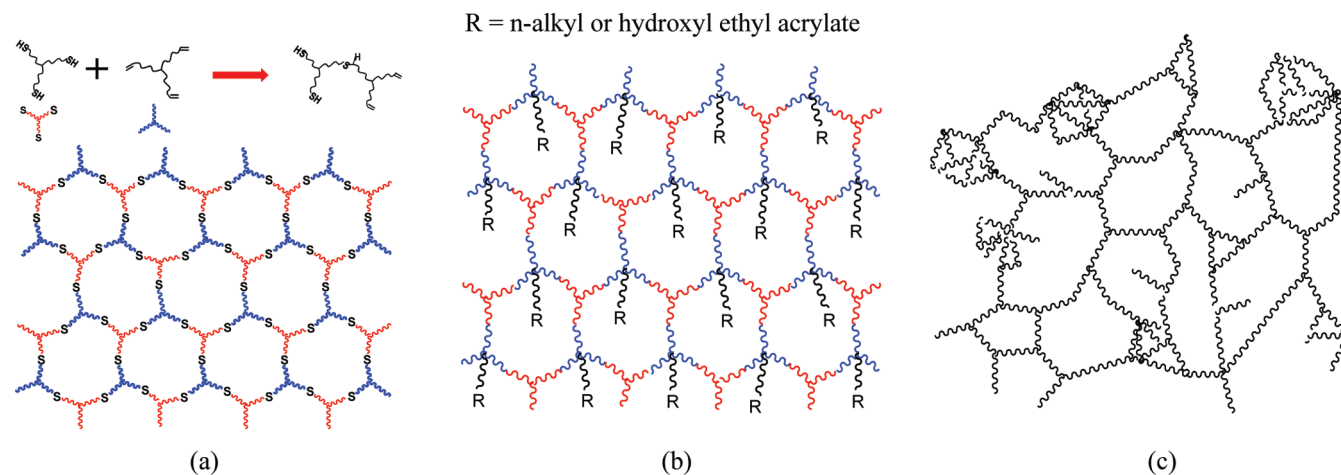
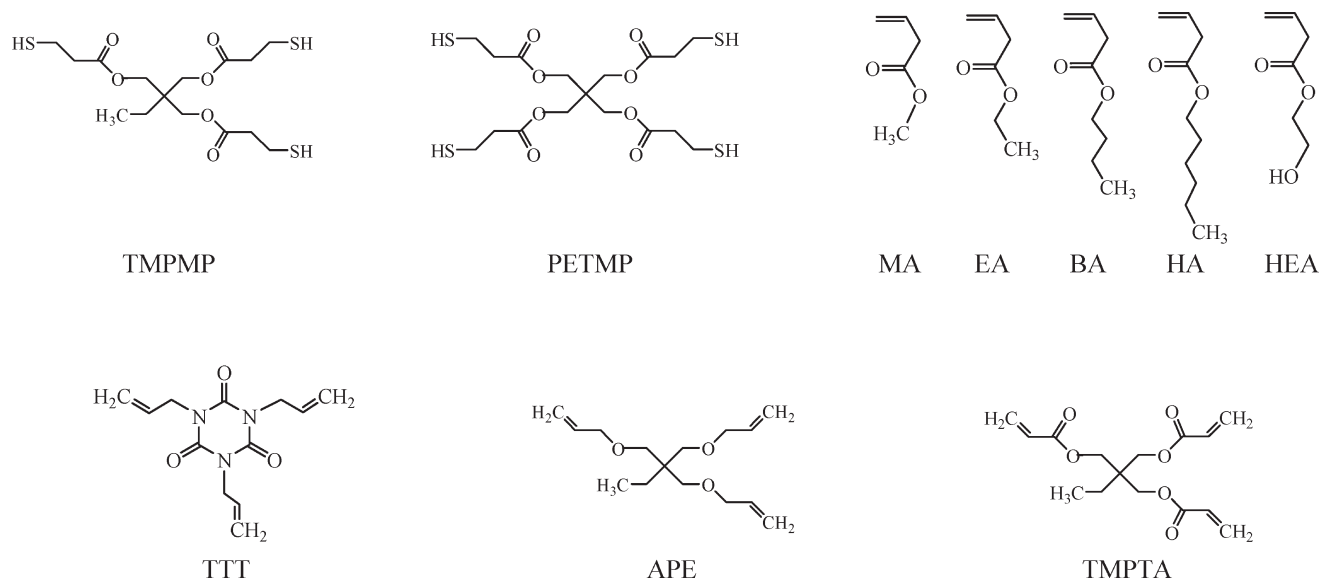


**Figure 1.** (a) Uniform and dense network structure of photopolymerized thiol-ene made with trithiol and triene, (b) modified thiol-ene networks with *n*-alkyl or hydroxyl ethyl acrylate and triene, and (c) inhomogeneous cross-linked structure of multifunctional acrylate homopolymer by forming microgel.

**Chart 1.** The molecular structures of thiols, enes, and acrylates

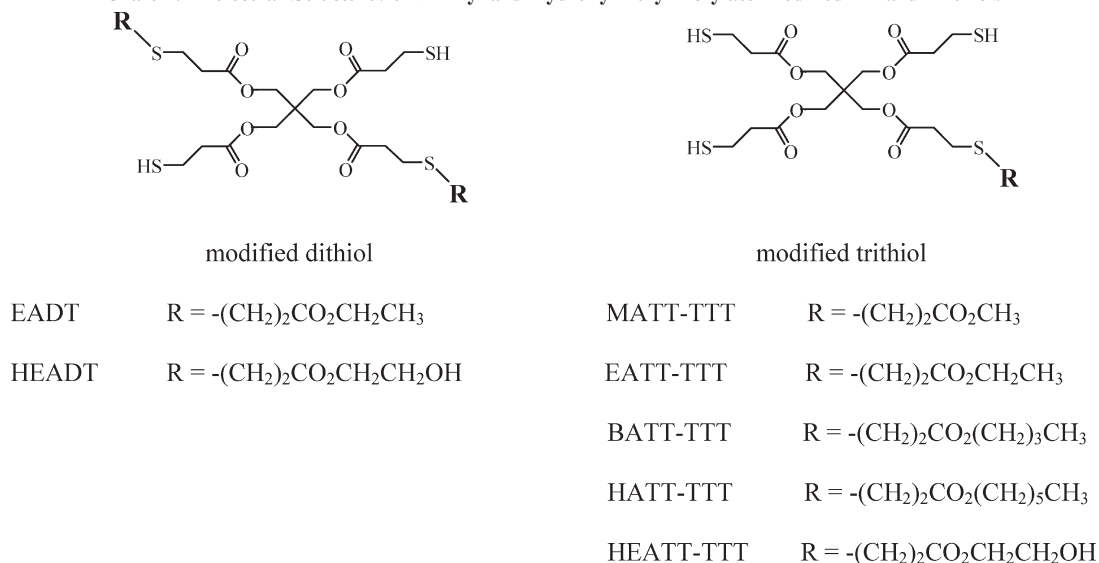


parameters can alter the physical phenomenon associated with cross-linked networks in general. In view of the reported effects for linear polymers of *n*-alkyl groups to induce motion below  $T_g$  and hydrogen bonding via hydroxyl groups to enhance heat capacity above  $T_g$ , we purport that such effects should also be effective in controlling sub- $T_g$  enthalpy relaxation in thiol-ene networks. This presents an excellent opportunity to not only corroborate a range of effects reported in the literature for linear polymers, but it also provides a systematic approach to defining chemical structural control of sub- $T_g$  relaxation phenomena for networks in general. Using the generalized format in Figure 1(b), *n*-alkyl (i.e., methyl, ethyl, butyl, and hexyl) acrylates and hydroxyl ethyl acrylate were used to functionalize thiol-ene networks, and the extent and rate of enthalpy relaxation was correlated to the heat capacity difference in the glassy and rubbery states and the corresponding enthalpic departure from equilibrium in the glassy phase as determined by  $\Delta C_p$ . In addition to the modification of thiol-ene networks by substituents, incorporating a third monomer<sup>35–39</sup> (multifunctional (meth)acrylate) that both copolymerizes (with thiol functional groups) and homopolymerizes is an effective method for altering the physical and mechanical properties of thiol-enes over a very broad range, thus leading to a new class of network architecture that combines the uniformity of thiol-ene networks with the heterogeneity of

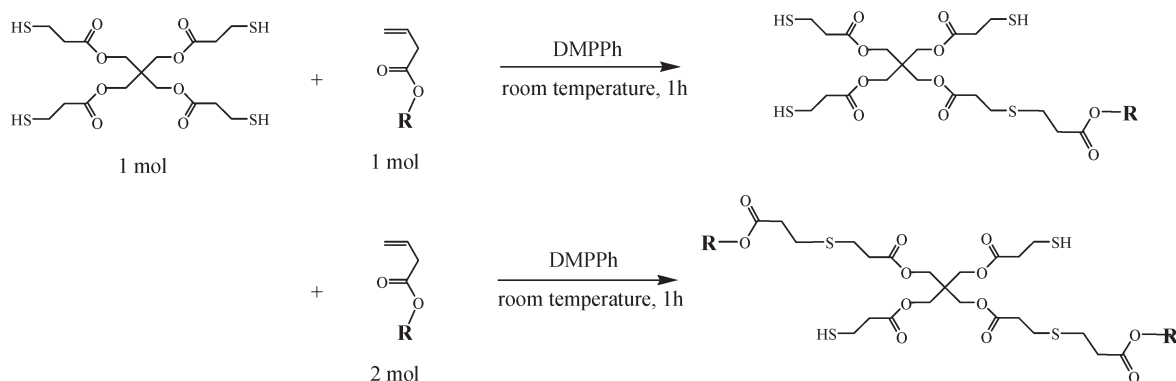
multifunctional acrylates. Unlike binary thiol-ene based systems which gel at relatively high conversions as dictated by the Flory-Stockmayer gel equation,<sup>40</sup> multiacrylates gel at much lower conversions (microgelation) and are characterized by very inhomogeneous networks and broad density distributions (Figure 1c).<sup>41–46</sup> The copolymerization of a multifunctional acrylate (i.e., TMPTA—trimethylolpropane triacrylate) with a thiol-ene system hinders the formation of the traditional thiol-ene uniform dense network structure, leading to a more inhomogeneous network with a broader cross-link density distribution. The appearance of defects in the network uniformity should affect the physical character of thiol-ene networks related to conformational degree of freedom, free volume, and ultimately relaxation processes. In this third approach, the rate and degree of enthalpy relaxation, as influenced by microgelation in the context of the thiol-ene network, was delineated with respect to changes in uniformity and  $\Delta C_p$  at  $T_g$ .

## Experimental Section

**Materials.** TMPMP (Triethylolpropane tris(3-mercaptopropionate), PETMP (pentaerythritol tetrakis(3-mercaptopropionate)),

Chart 2. Molecular Structures of *n*-Alkyl and Hydroxyl Ethyl Acrylate Modified Di- and Trithiols

Scheme 1. Overall Reaction Procedure for the Synthesis of modified Di- and Trithiols from PETMP and Acrylate Monomers



APE (allyl pentaerythritol), and TMPTA (trimethylolpropane triacrylate) were obtained from Bruno Bock Thio-Chemicals-S and Perstorp Specialty Chemicals, respectively. All *n*-alkyl and hydroxyl ethyl acrylates, TTT (1,3,5-triallyl-1,3,5-triazine-2,4,6(1*H*,3*H*,5*H*)-trione), and DMPPh (dimethyl phenyl phosphine) were purchased from Aldrich. The structures of all components and corresponding acronyms are shown in the Chart 1. The photoinitiator, 2,2-dimethoxy 2-phenyl acetophenone (DMPA), was supplied by Ciba Specialty Chemicals. All materials were used as received.

**Preparation of *n*-Alkyl/Hydroxyl Ethyl Acrylate Modified Thiols.** The basic structural units used to make the thiol–ene networks which are the subject of the investigation in this paper are shown in Charts 1 and 2. The three and four functional thiols, TMPMP and PETMP, and the two trifunctional enes, TTT and APE, in Chart 1 are standard multifunctional thiols and enes typically used to make thiol–ene networks. Several new difunctional and trifunctional thiols (modified di- and trithiols) shown in Chart 2 were made by the dimethylphenyl phosphine catalyzed reaction in Scheme 1 between the five acrylates in Chart 1 (MA, EA, BA, HA and HEA) and the PETMP. The thiol structures shown in Chart 2 are representative of the predominant chemical structure, with the samples actually consisting of a mixture of unsubstituted and multi-substituted components. *n*-Alkyl or hydroxyl ethyl acrylate modified trithiols were prepared through phosphine-catalyzed nucleophilic thiol Michael addition reaction to acrylates.<sup>47–50</sup> PETMP was first mixed with 0.1 wt % of DMPPh while nitrogen purging. *n*-Alkyl or hydroxyl ethyl acrylate was dripped

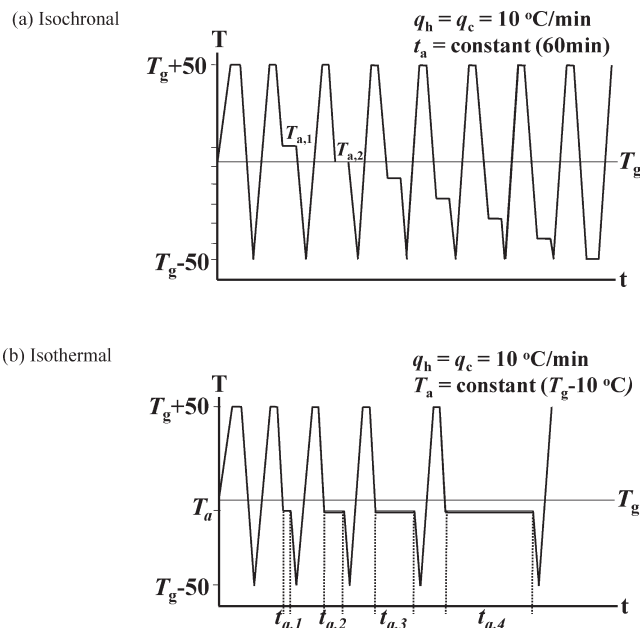


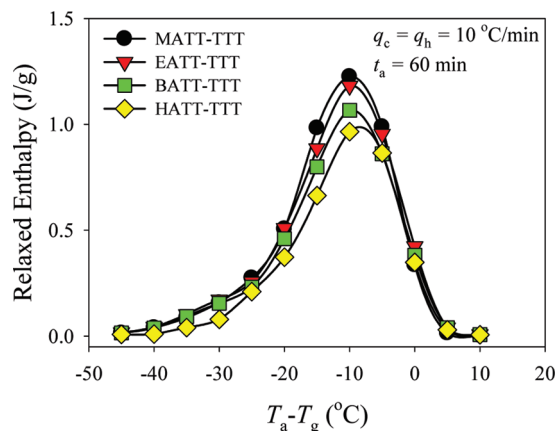
**Figure 2.** Schematic representation of two different annealing methods. The symbols  $q_h$  and  $q_c$  represent heating/cooling rates.

into the mixture for 10 min and the temperature was controlled below 30 °C with an ice bath in order to prevent acrylates

**Table 1.** Extent of Enthalpy Relaxation at 24 h ( $\Delta H_{24}$ ), Overall Relaxation Rate ( $\beta_H$ ),  $T_g$ ,  $T_{g,e} - T_{g,i}$ , and Assumed Maximum Enthalpy Relaxation ( $\Delta C_p \cdot \Delta T$ ) for Photopolymerized *n*-Alkyl Acrylate Modified Thiol–Ene Networks

sample no.	$\beta_H$ (J/g per decade)	$\Delta H_{24}$ (J/g)	$T_g$ (°C)	$\Delta C_p$ (J/g·°C)	$\Delta C_p \cdot \Delta T^a$ (J/g)	$T_{g,e} - T_{g,i}$ (°C)
MATT–TTT	1.18	2.32	9.8	0.47	4.75	10.9
EATT–TTT	1.15	2.26	6.2	0.46	4.59	12.0
BATT–TTT	1.06	2.09	−0.2	0.44	4.39	13.5
HATT–TTT	0.96	1.91	−3.2	0.40	3.99	14.5

$$^a \Delta T = |T_a - T_g| = 10\text{ °C}.$$

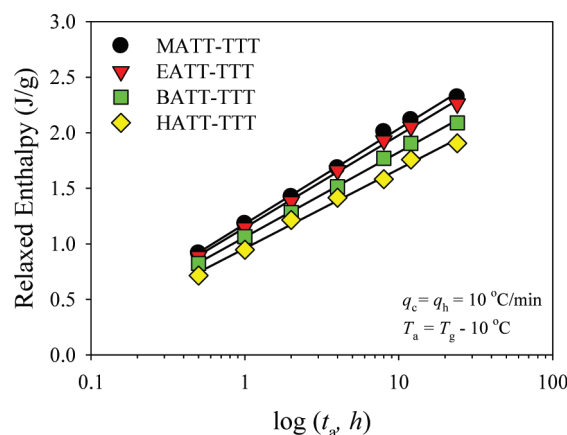
**Figure 3.** Enthalpy relaxation of photopolymerized *n*-alkyl acrylate modified trithiol–TTT networks as a function of the annealing temperature and alkyl chain length ( $q_h = q_c = 10\text{ °C/min}$ ,  $t_a = 60\text{ min}$ ).

from undergoing thermally initiated free-radical polymerization. 1:1 and 1:2 molar ratios between PETMP and acrylates were used for the modified trithiol and dithiol systems, respectively. After adding acrylates, the mixture was further reacted for 3 h at room temperature until all acrylates were consumed.

**Preparation of Thiol–Ene Network Films.** EATT–TTT and HEATT–TTT mixtures were photocured to produce thiol–ene networks. For thiol–ene–acrylate ternary systems, equimolar concentrations of TMPMP and APE were used for the thiol–ene binary network and the molar ratio of TMPMP to TMPMP–APE was varied from 0 to 100% to form ternary networks. A 1 wt % sample of DMPA was first dissolved in *n*-alkyl/hydroxyl ethyl acrylate modified di-/trithiol for modified thiol–ene systems and TMPMP for thiol–ene–acrylate ternary systems by sonication for 30 min. Thiol (–SH) and ene (–C=C–) concentrations were held constant at 1:1 equiv for all thiol–ene networks. Films were cast on glass plates (200  $\mu\text{m}$ ) and cured on a Fusion UV curing line system with a D bulb (400  $\text{W/cm}^2$ ) having a belt speed of 10 feet/min and irradiance of 3.1  $\text{W/cm}^2$ . All samples were postcured at 80 °C for 24 h to ensure complete reaction and eliminate any possibility of chemical conversion effect on enthalpy relaxation during sub- $T_g$  annealing.

**Characterization.** The thiol Michael addition reaction with PETMP and acrylates using DMPPH catalyst was monitored by FT-infrared (FTIR) spectroscopy and NMR. The complete disappearance of acrylate carbon double bonds was confirmed by peaks at 812  $\text{cm}^{-1}$  for FTIR, at 5.71 (q), 5.99 (q), and 6.23 (q) ppm for  $^1\text{H}$  NMR, and at 128.3 and 130.5 ppm for  $^{13}\text{C}$  NMR. A modified Bruker IFS 88 FTIR spectrometer was equipped with a horizontal sample accessory and thin samples (25  $\mu\text{m}$ ) were placed between two salt plates sealed with silicon in the FTIR. A small sample was taken every 30 min during reaction for FTIR measurements. After confirmation with FTIR, NMR measurements were conducted.  $^1\text{H}$  and  $^{13}\text{C}$  NMR spectra of *n*-alkyl/hydroxyl ethyl acrylate modified Di-/TriThiol were obtained on a Varian 300 MHz NMR in  $\text{CDCl}_3$  with tetramethylsilane (TMS) as the internal reference. FTIR and NMR spectra of the thiol Michael addition reaction with acrylate have been reported in the literature.<sup>47–50</sup>

Glass transition temperatures and enthalpy relaxation for all thiol–ene and modified thiol–ene networks were characterized with a TA Q1000 differential scanning calorimeter (DSC) with

**Figure 4.** Relaxed enthalpy ( $\delta_H$ ) vs logarithmic annealing time ( $t_a$ ) of photopolymerized *n*-alkyl acrylate modified trithiol–TTT networks ( $q_h = q_c = 10\text{ °C/min}$ ,  $T_a = T_g - 10\text{ °C}$ ).

RCS 90 (Refrigerated Cooling System). A RCS 90 cooling head mounted on the DSC Q1000 furnace encases the DSC cell preventing frost building-up during operation. Three calibration steps ( $T_{\text{zero}}$  calibration, enthalpy constant calibration, and Temperature calibration) for the TA Q1000 were performed periodically. Detailed calibration protocol has been well described in a previous literature.<sup>22</sup> The glass transition region and heat capacity change ( $\Delta C_p$ ) at  $T_g$  were characterized as described in the literature.<sup>51,52</sup> The beginning ( $T_{g,i}$ ) and end ( $T_{g,e}$ ) of the glass transition were determined as the temperature where the heat capacity starts to increase from the glassy phase and where it finally attains a constant value in the liquid state, respectively.  $T_g$  was defined by the temperature of the inflection point in the heat capacity versus temperature plot in the glass transition region.  $\Delta C_p$  was obtained by the heat capacity difference between the extrapolated lines of the glass and rubber heat capacities at  $T_g$ . Special attention was paid to running the DSC to ensure the accuracy of the enthalpy relaxation measurement. For two different annealing methods described in Figure 2, the measurement was conducted twice and the sequence of annealing was reversed in the second running. Equivalent results were obtained in each case; i.e., instrumental drift did not play a factor, and the results were reproducible despite the different order in obtaining the data sets. Furthermore, the heat flow and heat capacity of TMPMP–APE sample without aging, as a standard, were measured after every calibration and time-sequence scan to ensure consistency. Finally, in order to remove sampling errors, the same DSC pans (samples) were used for all measurements. All experiments were carried out under nitrogen with a flow rate of 50 mL/min. Sample weights were  $8.0 \pm 1.0\text{ mg}$  to ensure sufficient sensitivity for heat capacity measurements. DSC scans were conducted over the temperature range of  $\pm 50\text{ °C}$  from the glass transition region ( $T_{g,i} \sim T_{g,e}$ ). Annealing temperature ( $T_a$ ) and annealing time ( $t_a$ ) were controlled to establish different annealing methods. Detailed descriptions of measurement techniques are described in the text.

## Results and Discussion

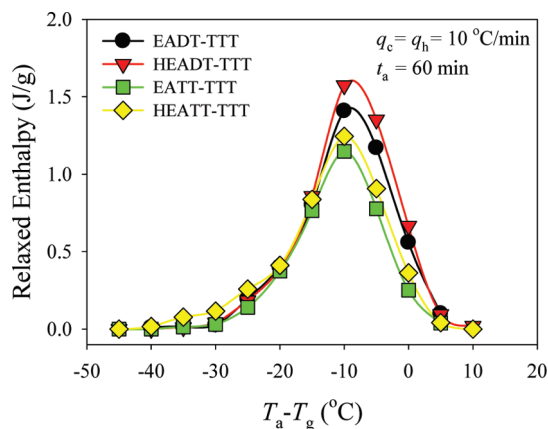
In this paper, we focus on defining the role of chemical structure of the basic thiol–ene networks and the modified thiol–ene and



**Table 2.** Extent of Enthalpy Relaxation at 24 h ( $\Delta H_{24}$ ), Overall Relaxation Rate ( $\beta_H$ ),  $T_g$ ,  $T_{g,e} - T_{g,i}$ , and Assumed Maximum Enthalpy Relaxation ( $\Delta C_p \cdot \Delta T$ ) for Photopolymerized Ethyl/Hydroxyl Ethyl Acrylate Modified Thiol–Ene Networks

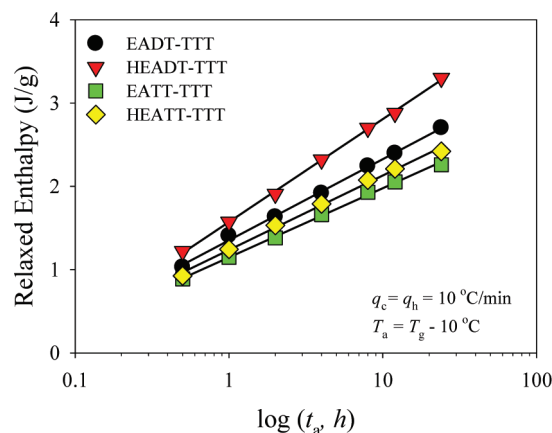
sample no.	$\beta_H$ (J/g per decade)	$\Delta H_{24}$ (J/g)	$T_g$ (°C)	$\Delta C_p$ (J/g·°C)	$\Delta C_p \cdot \Delta T^a$ (J/g)	$T_{g,e} - T_{g,i}$ (°C)
EADT–TTT	1.35	2.70	−26.8	0.54	5.45	11.8
HEADT–TTT	1.57	3.30	−14.0	0.62	6.24	15.7
EATT–TTT	1.15	2.26	6.2	0.46	4.59	11.3
HEATT–TTT	1.24	2.42	12.8	0.48	4.79	12.4

<sup>a</sup>  $\Delta T = |T_a - T_g| = 10$  °C.

**Figure 5.** Enthalpy relaxation of photopolymerized ethyl/hydroxyl ethyl acrylate modified di/trithiol–TTT networks as a function of the annealing temperature ( $q_h = q_c = 10$  °C/min,  $t_a = 60$  min).

modtrithiol–ene networks (see Charts 1 and 2 for component structures) on enthalpy relaxation. Sub- $T_g$  aging is both a temperature and time dependent physical phenomenon. Hence, the thiol–ene networks were equilibrated above  $T_g$  to remove prior thermal history and quenched to a temperature  $T_a$  ( $< T_g$ ), at which the aging process occurs. The subsequent enthalpy was monitored upon reheating a sample through its glass transition. Equilibration achieved by maintaining the sample for 10 min at a temperature above  $T_g$  ( $T_{g,e} + 50$  °C) effectively erases the previous thermal history, and is necessary in order to initialize the sample for physical aging. Enthalpy relaxation was studied by two different approaches whose schematic representations are shown in Figure 2: (a) *isochronal* and (b) *isothermal*.<sup>53</sup> The isothermal method provides information on the time dependency of the enthalpy relaxation processes, while the isochronal method assesses the temperature dependency of the relaxation processes.

***n*-Alkyl Acrylate Modified Thiol–Ene Networks.** To evaluate the effect of flexible alkyl side chains on the sub- $T_g$  annealing of thiol–ene networks, equimolar functional group mixtures of all of the MA, EA, BA, and HA modified trithiols in Chart 2 with TTT were photopolymerized. Thermal transitions of the resultant thiol–ene networks were characterized by DSC, and the results are summarized in Table 1. First, it is noted that the DSC glass transition breadth ( $T_{g,e} - T_{g,i}$ ) for four different *n*-alkyl acrylate modified thiol–ene networks is almost identical indicating that the uniformity of the thiol–ene networks is very high and not affected by the flexible *n*-alkyl substituent. Second, the glass transition temperature decreases progressively as the length of the *n*-alkyl chain on the modified trithiol–TTT network increases from methyl to hexyl, consistent with results observed for *n*-alkyl acrylate homopolymers where the longer more flexible *n*-alkyl chain acts as an internal plasticizer.<sup>30,32,54</sup> Concomitantly, the heat capacity change ( $\Delta C_p$ ) at  $T_g$  (see Table 1) also decreases as the number of methylene groups on the acrylate increases from methyl to hexyl. Hatakeyama et al.<sup>31</sup> has reported that side chain *n*-alkyl groups on linear polymer can sustain rotational

**Figure 6.** Relaxed enthalpy ( $\delta_H$ ) vs logarithmic annealing time ( $t_a$ ) of photopolymerized ethyl/hydroxyl ethyl acrylate modified di/trithiol–TTT networks ( $q_h = q_c = 10$  °C/min,  $T_a = T_g - 10$  °C).

motion below  $T_g$ , hence raising the specific heat capacity in the glassy state and thus lowering the change in heat capacity going from the glassy to rubbery state at  $T_g$ . We thus project that flexible *n*-alkyl side chains incorporated into thiol–ene networks also begin rotational motion at a temperature below  $T_g$ , thereby increasing the specific heat capacity below  $T_g$ , with the concomitant decrease in  $\Delta C_p$  with increase in the *n*-alkyl chain length (Table 1).

The *n*-alkyl acrylate modified trithiol–TTT networks were next annealed at specific temperatures ( $T_a$ –annealing temperature) every 5 °C from  $T_g + 10$  to  $T_g - 45$  °C for a time,  $t_a$  (60 min), to investigate the temperature dependency of enthalpy relaxation. The schematic diagram of the isochronal process is shown in Figure 2b. The extent of enthalpy relaxation was calculated from the difference thermograms using eq 1,<sup>22,55–57</sup>

$$\Delta H_r(T_a, t_a) = \int_{T_g - 50^\circ\text{C}}^{T_g + 50^\circ\text{C}} [C_p(T_a, t_a) - C_p(T_a, 0)] dT \quad (1)$$

where  $C_p(T_a, t_a)$  and  $C_p(T_a, 0)$  represent specific heat capacities for samples annealed at  $T_a$  for  $t = t_a$  and unannealed samples, respectively. The relaxed enthalpies as a function of  $T_a - T_g$  for all *n*-alkyl acrylate modified trithiol–TTT networks are shown in Figure 3. The asymmetric bell-shaped enthalpy relaxation curves occur over a narrow temperature range ( $\sim 20$  °C) with the maxima at about  $T_g - 10$  °C for each system, consistent with the results found for basic unmodified thiol–ene networks.<sup>22</sup> The position of the maxima are dictated by the relaxation rates which are set by a combination of the enthalpic departure from equilibrium and the characteristic enthalpic relaxation time at an annealing temperature ( $T_a$ ) for a given time ( $t_a$ , 60 min).<sup>22,58</sup> On the basis of the results in Figure 3, the extent of enthalpy relaxation at the peak maxima of each  $T_a - T_g$  versus relaxed enthalpy plot decreases as the *n*-alkyl chain length increases. If each sample is annealed at  $T_a - T_g = -10$  °C, the  $\Delta T_{\text{maximum}}$  for each network in Figure 3, the relaxed enthalpy

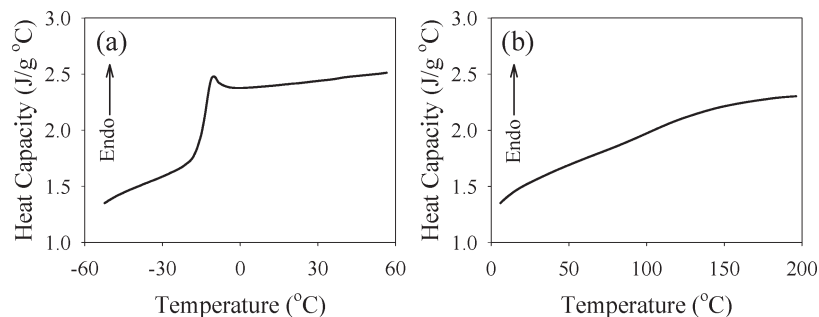


**Figure 7.** DSC heating scans of films of photopolymerized TMPMP-APE network (a) and TMPTA homopolymer (b) without annealing (cooling ( $q_c$ ) and heating rate ( $q_h$ ): 10 °C/min).

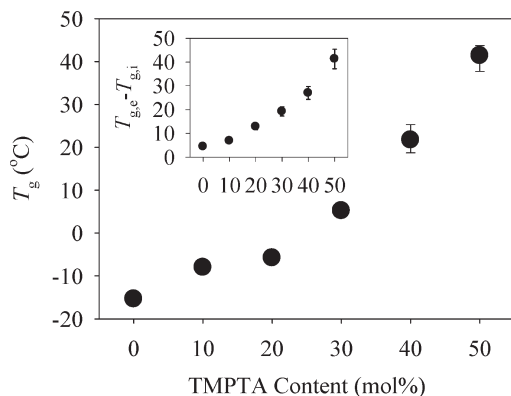


**Figure 8.** Effect of TMPTA on  $T_g$  of photopolymerized TMPMP-APE-TMPTA ternary system.

after 24 h ( $\Delta H_{24}$ ) can be obtained. As shown in Table 1, the  $\Delta H_{24}$  values also decrease with increasing  $n$ -alkyl chain length. Furthermore, the product of  $\Delta C_p$  and  $\Delta T$  ( $|T_a - T_g|$ ) in Table 1, where  $\Delta T = 10$  °C, also decreases with the  $n$ -alkyl chain length. The  $\Delta C_p \cdot \Delta T$  product is indicative of the ultimate departure of enthalpy from equilibrium conditions at the annealing temperature. Hence, based on the extent of enthalpy relaxation at the peak maximum in Figure 3, the value for  $\Delta H_{24}$ , and the  $\Delta C_p \cdot \Delta T$  product (Table 1), it can be concluded that the supposition of increased rotational motion afforded by increasing alkyl chain length in side chain substituent of linear polymers in the glassy phase<sup>30,31</sup> also applies to  $n$ -alkyl chain substituent in uniform thiol-ene networks.

Figure 4 shows the plot of enthalpy relaxation of  $n$ -alkyl acrylate modified trithiol-TTT networks as a function of annealing time ( $t_a$ ) at  $T_g - 10$  °C, the temperature where enthalpy relaxation exhibited a maximum during the isochronal analysis in Figure 3. The extent of enthalpy relaxation consistently increased with annealing time at  $T_a - T_g = -10$  °C and a linear relationship between the extents of enthalpy relaxation vs logarithmic annealing time is obtained. A simple quantitative method is used to analyze the general overall relaxation rate ( $\beta_H$ )<sup>22,59–62</sup> according to eq 2,

$$\beta_H = \frac{d\delta_H}{d[\log t_a]} \quad (2)$$

where  $\delta_H$  is the extent of enthalpy relaxation and  $t_a$  is the annealing time at  $T_a - T_g$ . The general overall relaxation rate ( $\beta_H$ ) obtained by the slopes of each plot in Figure 4 (see Table 1) shows that the enthalpy relaxation rate of  $n$ -alkyl acrylate modified trithiol-TTT networks decreases with the length of  $n$ -alkyl acrylate substituent, consistent with the decrease in departure of the enthalpy from equilibrium as

defined by the  $\Delta C_p \cdot \Delta T$  product in Table 1. It is clear that the smaller excess enthalpy obtained by incorporating flexible  $n$ -alkyl acrylates into the thiol-ene networks results in a slower overall enthalpy relaxation rate ( $\beta_H$ ), corroborating the results found for  $\Delta H_{24}$ .

#### Hydroxyl Alkyl Acrylate Modified Thiol-ene Networks.

The hydrogen bonding effect on enthalpy relaxation was next investigated by comparing networks formed from HEATT-TTT, EATT-TTT, HEADT-TTT, and EADT-TTT systems (see Chart 2 for description of components). Results of the basic DSC heating scans,  $T_g$ s and  $\Delta C_p$ s, are summarized in Table 2. According to the speculation in the Introduction based on linear polymers,<sup>31,33,34</sup> the HEADT-TTT and HEATT-TTT networks have higher  $T_g$ s and  $\Delta C_p$  values than for the EADT-TTT and EATT-TTT networks. The increase in  $T_g$  and  $\Delta C_p$  is more pronounced for the HEADT-TTT based networks since the effect of hydrogen bonding would be expected to be more effective in a system of lower chemical cross-link density. The higher  $\Delta C_p$  values at  $T_g$  for the hydrogen bonding networks containing HEA mainly results from the onset of contributions from hydrogen bonding to the heat capacity at temperatures greater than  $T_g$  (rubbery state). In other words, hydrogen bonding opens up another mode (breaking or bending of hydrogen bonds) for dissipation of the thermal energy needed to increase temperature in the rubbery state in addition to translational, rotational, and vibrational contributions to the heat capacity.<sup>31,33,34,63</sup>

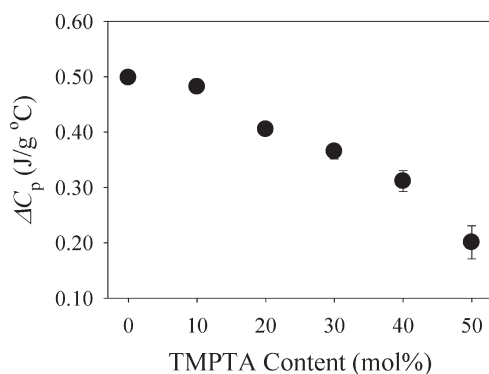
The effect of hydrogen bonding on temperature and time dependency of enthalpy relaxation were next investigated using isochronal and isothermal DSC measurements. In Figure 5, the relaxed enthalpies as a function of  $T_a - T_g$  for the HEADT-TTT and HEATT-TTT networks obtained using eq 1 are seen to exhibit peak maxima at  $T_g - 10$  °C similar to that observed for EADT-TTT-ene and EATT-TTT-ene networks, with the caveat that the extent of enthalpy relaxation of the networks from HEADT-TTT and HEATT-TTT are higher than the corresponding EADT-TTT and EATT-TTT networks. In order to more clearly characterize the effect of hydrogen bonding on enthalpy relaxation, isothermal annealing measurements were conducted. On the basis of the general overall relaxation rate ( $\beta_H$ ) and  $\Delta H_{24h}$  (Figure 6 and Table 2), it is obvious that the enthalpy relaxation rates for thiol-ene networks is enhanced by incorporating hydrogen bonding, consistent with the values for  $\Delta C_p \cdot \Delta T$  (Table 2), an estimate for the enthalpic departure from equilibrium at the annealing temperature. The greater incremental increase in  $\Delta C_p \cdot \Delta T$  and  $\Delta H_{24h}$  for the HEADT-TTT network compared to the HEATT-TTT network results from the lower chemical network cross-link density for the dithiol-based networks.

**TMPMP-APE-TMPTA Ternary System.** Thiol-ene-acrylate ternary systems were next used to investigate the effect

**Table 3. Extent of Enthalpy Relaxation at 24 h ( $\Delta H_{24}$ ), Overall Relaxation Rate ( $\beta_H$ ),  $T_g$ ,  $T_{g,e} - T_{g,i}$ , and Assumed Maximum Enthalpy Relaxation ( $\Delta C_p \cdot \Delta T$ ) for Photopolymerized TMPMP–APE–TMPTA Ternary System**

sample no.	$\beta_H$ (J/g per decade)	$\Delta H_{24}$ (J/g)	$T_g$ (°C)	$\Delta C_p$ (J/g·°C)	$\Delta C_p \cdot \Delta T^a$ (J/g)	$T_{g,e} - T_{g,i}$ (°C)
TS-APE	1.46	3.25	−15.1	0.50	4.99	4.0
TMPMP-APE-10 mol % TMPTA	1.34	3.01	−8.1	0.48	4.82	6.2
TMPMP-APE-20 mol % TMPTA	1.02	2.19	5.7	0.41	4.05	11.5
TMPMP-APE-30 mol % TMPTA	0.79	1.74	5.2	0.37	3.65	17.3
TMPMP-APE-40 mol % TMPTA	0.64	1.40	21.1	0.31	3.12	24.3
TMPMP-APE-50 mol % TMPTA	0.48	1.02	42.9	0.24	2.44	37.2
TMPMP-APE-60 mol % TMPTA	0.32	0.73	ND <sup>b</sup>	ND <sup>b</sup>	ND <sup>b</sup>	ND <sup>b</sup>

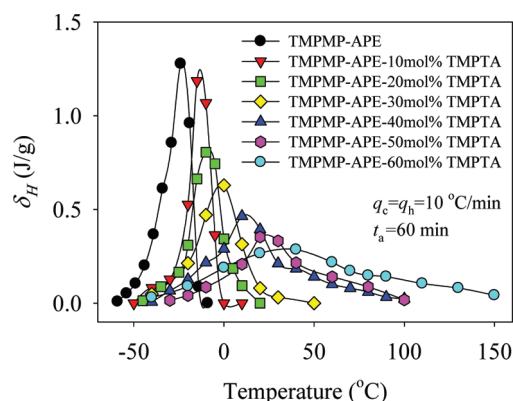
<sup>a</sup>  $\Delta T = |T_a - T_g| = 10$  °C. <sup>b</sup> Not defined by DSC.

**Figure 9.** Effect of TMPTA on heat capacity of photopolymerized TMPMP–APE–TMPTA ternary system.

of network uniformity on sub- $T_g$  aging. Figure 7 shows the DSC heating scans and glass transition for the photopolymerized binary TMPMP–APE network and TMPTA homopolymer. As discussed already, due to the network uniformity, TMPMP–APE has a very narrow glass transition temperature region and a distinct enthalpy relaxation peak around  $T_g$  obtained by DSC scanning of the precooled sample at 10 °C/min cooling ( $q_c$ ) followed by an immediate (no time for extended aging at a single annealing temperature) subsequent heating at a rate ( $q_h$ ) of 10 °C/min (Figure 7a). Concomitantly, photopolymerized TMPTA has an inhomogeneous cross-linked structure with a wide variation of cross-link densities and corresponding microgel structures,<sup>41–46</sup> as well as dangling chain ends,<sup>6,35</sup> resulting in a very broad glass transition region and no clearly defined enthalpy relaxation peak (Figure 7b).

To define the effect of sub- $T_g$  annealing of ternary thiol–ene–acrylate networks, systems were prepared by mixing TMPMP–APE with increasing TMPTA concentrations (10, 20, 30, 40, 50, and 60 mol %). The basic DSC glass transition temperature and breadth ( $T_{g,e} - T_{g,i}$ ) increases as a function of TMPTA content (Figure 8 and Table 3). It is clear that incorporating TMPTA into the thiol–ene network successfully decreases the network uniformity due to the microgel formation by TMPTA homopolymerization, acting like rigid amorphous region, restricts molecular mobility of thiol–ene networks, consistent with previous reports for other ternary thiol–ene–(meth)acrylate systems.<sup>6,35</sup>

The restriction of molecular mobility in the thiol–ene network by incorporation of the third component leads to a reduction of  $\Delta C_p$  values. As shown in Figure 9,  $\Delta C_p$  at  $T_g$  of TMPMP–APE–TMPTA also significantly decreases as a function of TMPTA content due to restriction of internal degrees of freedom resulted from the microgelation of TMPTA accompanied by broadened distribution of network/cross-link density and consequent broad glass transition temperature range and distribution of relaxation times. The restriction of molecular mobility above  $T_g$  which reduces the heat capacity in the rubbery phase, obviously results in a decrease in the relaxed enthalpy after

**Figure 10.** Temperature dependency of enthalpy relaxation of photopolymerized TMPMP–APE–TMPTA ternary system ( $q_c = q_h = 10$  °C/min,  $t_a = 60$  min).

24 h ( $\Delta H_{24h}$ ) as well as ultimate enthalpy relaxation ( $\Delta C_p \cdot \Delta T$ ) as a function of TMPTA content as shown in Table 3.

The broadening of the temperature range and restrictive effect on enthalpy relaxation by incorporating TMPTA into the TMPMP–APE network is even more obvious when characterized by temperature dependent (isochronal) analysis (Figure 10) and time-dependency (isothermal) measurements (Figure 11 and 12). The relaxed enthalpy ( $\delta_H$ ) versus sub- $T_g$  aging temperature for TMPMP–APE–TMPTA ternary films in Figure 10 obtained by eq 1 using isochronal analysis clearly exhibits a dramatic broadening and decrease in  $\delta_H$  at a given temperature below  $T_g$  as a function of TMPTA content, consistent with the decrease in  $\Delta C_p \cdot \Delta T$ , the enthalpic departure from equilibrium at the annealing temperature. Interestingly, the maximum values for  $\delta_H$  for all TMPMP–APE–TMPTA samples are still observed at about  $T_g - 10$  °C, consistent with results for the *n*-alkyl/hydroxyl ethyl acrylate modified thiol–ene networks discussed in previous sections and reported for several binary thiol–ene systems.<sup>22</sup> In Figure 11, the overshoot effect for enthalpy relaxation decreases progressively with increasing TMPTA content. The overall enthalpy relaxation rate ( $\beta_H$ ) obtained from the slopes of the plots in Figure 12 in Table 3 decreases as a function of TMPTA content indicating that  $\beta_H$  is affected by inclusion of the third monomer (TMPTA) in the TMPMP–APE network, i.e., the multifunctional acrylate both copolymerizes (with TMPMP) and homopolymerizes thereby decreasing the network uniformity and reducing the physical aging process. In other words, the enthalpy relaxation is not concentrated over a narrow temperature breadth.

## Conclusions

Thiol–ene networks were chemically modified to provide unprecedented control of enthalpy relaxation via three methods: incorporation of (1) *n*-alkyl side chains, (2) hydrogen bonding hydroxyl substituents, and (3) a third (acrylate) component (ternary system). *n*-Alkyl and hydroxyl side chain groups were

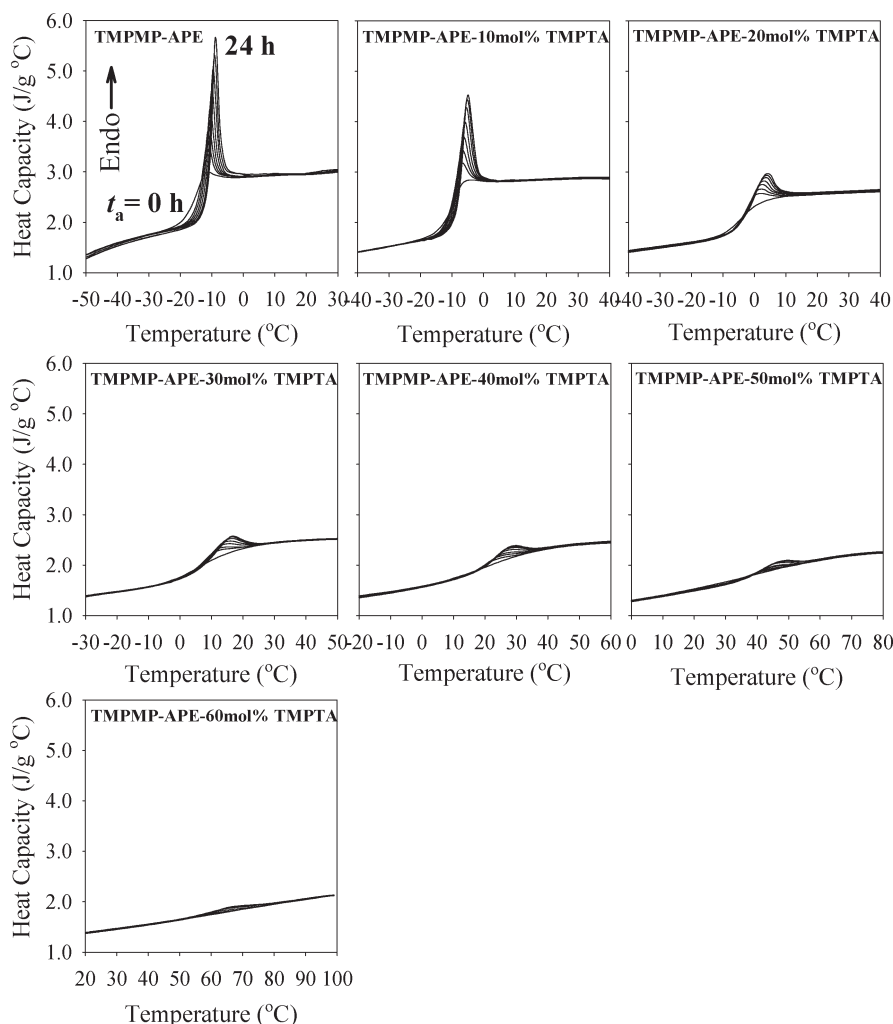


**Figure 11.** DSC heating scans of photopolymerized TMPMP–APE–TMPTA ternary system as a function of annealing time ( $t_a$ ) ( $q_c = q_h = 10^\circ\text{C}/\text{min}$ ,  $T_a = T_g - 10^\circ\text{C}$ ).

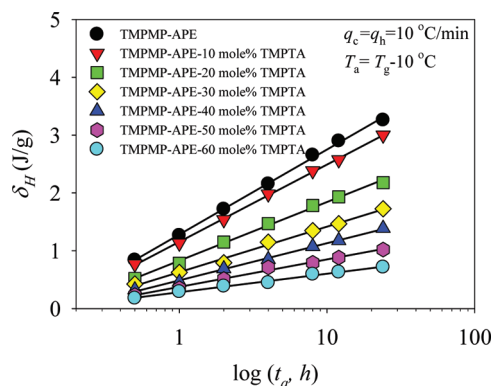


**Figure 12.** Relaxed enthalpy ( $\delta_H$ ) vs logarithmic annealing time ( $t_a$ ) of photopolymerized TMPMP–APE–TMPTA ternary system ( $q_c = q_h = 10^\circ\text{C}/\text{min}$ ,  $T_a = T_g - 10^\circ\text{C}$ ).

incorporated into the network using chemically modified multifunctional thiols to investigate the effect of flexible alkyl side chains and hydrogen bonding on enthalpy relaxation of thiol–ene networks without sacrificing their characteristic network uniformity. In all of the modified networks, the breadth of the glass transition temperature was not affected by the side chain appendages since the base cross-link density and network chemical structure was not altered.  $T_g$ ,  $\Delta C_p$ , and  $\Delta H_{24}$  decrease with an increase in the length of the alkyl chain due to the internal plasticizing effect of flexible alkyl

side chains. Hydrogen bonding by hydroxyl substituents requires additional enthalpy involved in long-range segmental motions leading to higher heat capacity differences at  $T_g$  and, as a resultant, a larger extent of enthalpic deviation from equilibrium at temperature below  $T_g$ . For the networks with appended alkyl and hydroxyl side groups, the rate of enthalpy relaxation at a specific temperature below  $T_g$  was found to be directly related to the deviation from enthalpic equilibrium as determined by the product  $\Delta C_p \cdot \Delta T$ . Multifunctional acrylate (TMPTA) was also incorporated into the thiol–ene network structure to investigate the effect of the network uniformity on physical aging behavior. The extent of enthalpy relaxation decreased and the distribution was drastically broadened as a function of TMPTA content. It is concluded that network uniformity is a critical factor affecting sub- $T_g$  relaxation of thiol–ene based networks. In addition, the restrictive effect of the rigid amorphous region by microgelation of TMPTA homopolymerization results in decreasing the enthalpic relaxation rate and corresponding extent of the relaxed enthalpy in 24 h ( $\Delta H_{24h}$ ) based on the decrease in the enthalpic deviation from equilibrium at the annealing temperature ( $\Delta C_p \cdot \Delta T$ ).

**Acknowledgment.** We acknowledge Perstorp, Bruno Bock, and Ciba Specialty Chemicals for materials and Fusion UV Systems for the light source.

## References and Notes

- (1) Hoyle, C. E.; Lee, T. Y.; Roper, T. J. *Polym. Sci., Part A: Polym. Chem.* **2004**, 42, 5301.



- (2) Cramer, N. B.; Bowman, C. N. *J. Polym. Sci., Part A: Polym. Chem.* **2001**, *39*, 3311.
- (3) Cramer, N. B.; Reddy, S. K.; Cole, M.; Hoyle, C. E.; Bowman, C. N. *J. Polym. Sci., Part A: Polym. Chem.* **2004**, *42*, 5817.
- (4) Khire, V. S.; Harant, A. W.; Watkins, A. W.; Anseth, K. S.; Bowman, C. N. *Macromolecules* **2006**, *39*, 5081.
- (5) Senyurt, A. F.; Hoyle, C. E.; Wei, H.; Piland, S. G.; Gould, T. E. *Macromolecules* **2007**, *40*, 3174.
- (6) Wei, H.; Senyurt, A. F.; Jönsson, S.; Hoyle, C. E. *J. Polym. Sci., Part A: Polym. Chem.* **2007**, *45*, 822.
- (7) Roper, T. M.; Guymon, C. A.; Jönsson, E. S.; Hoyle, C. E. *J. Polym. Sci., Part A: Polym. Chem.* **2004**, *42*, 6283.
- (8) Lee, T. Y.; Roper, T. M.; Jönsson, E. S.; Guymon, C. A.; Hoyle, C. E. *Macromolecules* **2004**, *37*, 3606.
- (9) Li, Q.; Zhou, H.; Wicks, D. A.; Hoyle, C. E. *J. Polym. Sci., Part A: Polym. Chem.* **2007**, *45*, 5103.
- (10) Wei, H.; Li, Q.; Ojelade, M.; Madbouly, S.; Otaigbe, J. U.; Hoyle, C. E. *Macromolecules* **2007**, *40*, 8788.
- (11) Senyurt, A. F.; Warren, G.; Whitehead, J. B.; Hoyle, C. E. *Polymer* **2006**, *47*, 2741.
- (12) Moran, I. W.; Briseno, A. L.; Loser, S.; Carter, K. R. *Chem. Mater.* **2008**, *20*, 4595.
- (13) Yi, Y. W.; Khire, V.; Bowman, C. N.; MacLennan, J. E.; Clark, N. A. *J. Appl. Phys.* **2008**, *103*, 6.
- (14) Good, B. T.; Reddy, S.; Davis, R. H.; Bowman, C. N. *Sensors Actuators B: Chem.* **2007**, *120*, 378.
- (15) Pojman, J. A.; Varisli, B.; Perryman, A.; Edwards, C.; Hoyle, C. E. *Macromolecules* **2004**, *37*, 691.
- (16) Khire, V. S.; Benoit, D. S. W.; Anseth, K. S.; Bowman, C. N. *J. Polym. Sci., Part A: Polym. Chem.* **2006**, *44*, 7027.
- (17) Khire, V. S.; Harant, A. W.; Watkins, A. W.; Anseth, K. S.; Bowman, C. N. *Macromolecules* **2006**, *39*, 5081.
- (18) Dickey, M. D.; Collister, E.; Raines, A.; Tsiartas, P.; Holcombe, T.; Sreenivasan, S. V.; Bonnacaze, R. T.; Willson, C. G. *Chem. Mater.* **2006**, *18*, 2043.
- (19) Fox, A. E.; Fontecchio, A. K. *Appl. Phys. Lett.* **2007**, *91*, 3.
- (20) Campos, L. M.; Meinel, I.; Guino, R. G.; Scheirhorn, M.; Gupta, N.; Stucky, G. D.; Hawker, C. J. *Adv. Mater.* **2008**, *20*, 3728.
- (21) Sangermano, M.; Gross, S.; Priola, A.; Rizza, G.; Sada, C. *Macromol. Chem. Phys.* **2007**, *208*, 2560.
- (22) Shin, J.; Nazarenko, S.; Hoyle, C. E. *Macromolecules* **2008**, *41*, 6741.
- (23) Lin, Y. G.; Sauterreau, H.; Pascault, J. P. *J. Appl. Polym. Sci.* **1986**, *32*, 4595.
- (24) Lee, A.; McKenna, G. B. *Polymer* **1988**, *29*, 1812.
- (25) Huang, D.; Yang, Y.; Zhuang, G.; Li, B. *Macromolecules* **1999**, *32*, 6675.
- (26) Huang, D.; Yang, Y.; Zhuang, G.; Li, B. *Macromolecules* **2000**, *33*, 461.
- (27) Privalko, V. P.; Demchenko, S. S.; Lipatov, Y. S. *Macromolecules* **1986**, *19*, 901.
- (28) Andreatti, L.; Faetti, M.; Giordano, M.; Zulli, F. *Macromolecules* **2005**, *38*, 6056.
- (29) Mark, J. E.; Erman, B. *Elastomeric Polym. Network*, Prentice Hall, Inc.: NJ, 1992.
- (30) Mays, J. W.; Siakali-Kioulafa, E.; Hadjichristidis, N. *Macromolecules* **1990**, *23*, 3530.
- (31) Hatakeyama, T.; Hatakeyama, H. *Thermochim. Acta* **1995**, *267*, 249.
- (32) Cypcar, C. C.; Camelio, P.; Lazzeri, V.; Mathias, L. J.; Waegell, B. *Macromolecules* **1996**, *29*, 8954.
- (33) Schroeder, M. J.; Roland, C. M.; Kwei, T. K. *Macromolecules* **1999**, *32*, 6249.
- (34) McGonigle, E. A.; Cowie, J. M. G.; Arrighi, V.; Pethrick, R. A. *J. Mater. Sci.* **2005**, *40*, 1869.
- (35) Senyurt, A. F.; Wei, H.; Phillips, B.; Cole, M.; Nazarenko, S.; Hoyle, C. E.; Piland, S. G.; Gould, T. E. *Macromolecules* **2006**, *39*, 6315.
- (36) Lee, T. Y.; Smith, Z.; Reddy, S. K.; Reddy, S. K.; Cramer, N. B.; Bowman, C. N. *Macromolecules* **2007**, *40*, 1466.
- (37) Lee, T. Y.; Carioscia, J.; Smith, Z.; Bowman, C. N. *Macromolecules* **2007**, *40*, 1473.
- (38) Rydholm, E.; Held, N. L.; Bowman, C. N.; Anseth, K. S. *Macromolecules* **2006**, *39*, 7882.
- (39) Carioscia, J. A.; Stansbury, J. W.; Bowman, C. E. *Polymer*, **2007**, *48*.
- (40) Jacobian, A. F. In *Radiation Curing in Polymer Science and Technology III*; Fouassier, J. D.; Rabek, J. F., Eds; Elsevier: London, 1993; Chapter 7.
- (41) Boots, H. M. J.; Kloosterboer, J. G.; van de Hei, G. M. M. *Br. Polym. J.* **1985**, *17*, 219.
- (42) Elliott, J. E.; Bowman, C. N. *Macromolecules* **1999**, *32*, 8621.
- (43) Lovestead, T. M.; Bowman, C. N. *Macromolecules* **2005**, *38*, 4913.
- (44) Kloosterboer, J. G.; Lijten, G. F. C. M.; Boots, H. M. J. *Makromol. Chem., Macromol. Symp.* **1989**, *24*, 223.
- (45) Bowman, C. N.; Anseth, K. S. *Macromol. Symp.* **1995**, *93*, 269.
- (46) Kannurpatti, A. R.; Anseth, J. W.; Bowman, C. N. *Polymer* **1998**, *39*, 2507.
- (47) Lee, T. Y.; Kaung, W.; Jonsson, E. S.; Lowery, K.; Guymon, C. A.; Hoyle, C. E. *J. Polym. Chem.: Part A: Polym. Chem.* **2004**, *42*, 4424.
- (48) Kilambi, H.; Stansbury, J. W.; Bowman, C. N. *J. Polym. Chem.: Part A: Polym. Chem.* **2008**, *46*, 3452.
- (49) Chan, J. W.; Yu, B.; Hoyle, C. E.; Lowe, A. B. *Chem. Commun.* **2008**, 4959.
- (50) Shin, J.; Matsushima, H.; Chan, J. W.; Hoyle, C. E. *Macromolecules* **2009**, *42*, 3294.
- (51) Cheng, S. Z. D.; Cao, M.-Y.; Wunderlich, B. *Macromolecules* **1986**, *19*, 1868.
- (52) Mathot, B. F. *Calorimetry and Thermal Analysis of Polymers*, Hanser: Munich, Germany, 1993.
- (53) Cerrada, M. L.; McKenna, G. B. *Macromolecules* **2000**, *33*, 3065.
- (54) Sperling, L. H. *Introduction to Physical Polymer Science*, John Wiley & Sons, Inc.: New York, 1992.
- (55) Pellerin, C.; Pelletier, I.; Pezolet, M.; Prud'homme, R. R. *Macromolecules* **2003**, *36*, 153.
- (56) Roe, R.-J.; Millman, G. M. *Polym. Eng. Sci.* **1983**, *23*, 318.
- (57) Montserrat, S.; Calventus, Y.; Hutchinson, J. M. *Prog. Org. Coat.* **2006**, *55*, 35.
- (58) Gedde, U. W. *Polymer Physics*; Chapman & Hall: London, 1995.
- (59) Hutchinson, J. M. *Prog. Polym. Sci.* **1995**, *20*, 703.
- (60) Pan, P.; Zhu, B.; Inoue, Y. *Macromolecules* **2007**, *40*, 9664.
- (61) Struik, L. C. E. *Polymer* **1987**, *28*, 1869.
- (62) Struik, L. C. E. *Physical Aging in Amorphous Polymers and Other Materials*; Elsevier Publishing Company: New York, 1978.
- (63) Cooper, A. *Biophys. Chem.* **2000**, *85*, 25.